

A SELF-ADAPTIVE ENHANCED VIBRATING PARTICLE SYSTEM ALGORITHM FOR CONTINUOUS OPTIMIZATION PROBLEMS

M. Paknahad¹, P. Hosseini^{1*,†} and A. Kaveh²

¹*Faculty of Engineering, Mahallat Institute of Higher Education, Mahallat, Iran*

²*School of Civil Engineering, Iran University of Science and Technology, Narmak, Tehran, Iran*

ABSTRACT

Optimization methods are essential in today's world. Several types of optimization methods exist, and deterministic methods cannot solve some problems, so approximate optimization methods are used. The use of approximate optimization methods is therefore widespread. One of the metaheuristic algorithms for optimization, the EVPS algorithm has been successfully applied to engineering problems, particularly structural engineering problems. As this algorithm requires experimental parameters, this research presents a method for determining these parameters for each problem and a self-adaptive algorithm called the SA-EVPS algorithm. In this study, the SA-EVPS algorithm is compared with the EVPS algorithm using the 72-bar spatial truss structure and three classical benchmarked functions

Keywords: enhanced vibrating particle system; self-adaptive algorithm; SA-EVPS algorithm; metaheuristic algorithms; continuous optimization problems.

Received: 20 September 2022; Accepted: 26 November 2022

1. INTRODUCTION

Optimization leads to the efficient use of funds, time, and materials in engineering. It is common to use metaheuristic algorithms to solve problems in a short amount of time, but they cannot guarantee that the best solution will be obtained. In order to provide more efficient answers in a reasonable amount of time, metaheuristic algorithms present methods that result in more efficient answers for various problems. Over the last two decades, metaheuristic optimization techniques have become very popular. The following are a few of

*Corresponding author: Faculty of Engineering, Mahallat Institute of Higher Education, Mahallat, Iran

†E-mail address: P.Hosseini@mahallat.ac.ir (P. Hosseini)

these methods:

Genetic Algorithm (GA) [1], Charged System Search (CSS) [2], Colliding Bodies Optimization (CBO) [3], Tug of War Optimization (TWO) [4], Accelerated Water Evaporation Optimization (AWEO) [5], Dolphin Echolocation optimization (DE) [6], Simplified Dolphin Echolocation optimization (SDE)[7], Modified Dolphin Monitoring (MDM) [8], Differential evolution algorithm (DE) [9], League Championship Algorithm (LCA) [10], Teaching Learning Based Optimization (TLBO) [11], Chemical Reaction Optimization (CRO) [12], Sine Cosine Algorithm (SCA) [13], Search and Rescue Optimization Algorithm (SSOA) [14], Water Wave Optimization (WWO) [15], Honey Badger Algorithm (HBA) [16].

Metaheuristic algorithms were quite simple at first, and were usually inspired by very simple concepts. Typically, inspiration comes from physical phenomena, animal behavior, or evolutionary concepts [17]. Simple metaheuristic algorithms can be simulated, proposed, hybridized, or improved by computer scientists. As a result, other scientists can learn and apply metaheuristic algorithms quickly. A metaheuristic is flexible if it can be applied to different problems without requiring any special changes in its structure. Unlike other methods, metaheuristic algorithms tend to assume problems as black boxes. Metaheuristic algorithms consider only inputs and outputs of a system. Designers need only know how to represent their problems for metaheuristic algorithms. Most metaheuristic algorithms are not derivation-based. Metaheuristic algorithms optimize problems stochastically, unlike gradient-based optimization. To find the optimum, the optimization process starts with random solutions. Metaheuristic algorithms are highly appropriate for problems with expensive derivatives or unknowns. Metaheuristic algorithms are better than conventional optimization techniques at avoiding local optima. Metaheuristic algorithms are stochastic, thus avoiding local stagnation and searching the entire search space extensively [17]. In real problems, the search space is often unknown and complex with many local optima, which is why metaheuristic algorithms can be useful.

The Vibrating Particle Systems (VPS) algorithm models viscous damping for a single degree of freedom system [18]. The purpose of this algorithm is to investigate the gradual movement of particles towards their equilibrium position. In order to improve the performance of VPS, the EVPS algorithm was developed by changing some parameters of the VPS algorithm [19]. A number of optimization problems have been solved using the EVPS algorithm, some of which are listed below:

Hosseini Vaez et al. developed an optimization problem to calculate the reliability index for structural problems with implicit limit state functions, in order to reduce the computation effort [20]. An integrated dynamic extended finite element method (XFEM) based on geometry-based crack detection for plate structures has been presented by Fathi et al. [21]. According to Kaveh et al, the Modified Dolphin Monitoring (MDM) operator was applied to the EVPS algorithm to evaluate the reliability index of three well-known steel frame structures [22]. The purpose of Kaveh et al's study was to improve the EVPS algorithm by reducing the regulatory parameters' impact on the algorithm's performance [23]. To reduce the burden of calculations associated with the former methods of damage detection, Kaveh et al presented a new objective function to detect damage. In the first phase, natural frequencies are calculated, and in the second phase, mode shapes are evaluated [24]. As part

of a two-step approach, Hosseini Vaez et al. optimized reliability-based structures by examining the probabilistic constraint if the deterministic constraint was satisfied [25]. Using nonlinear time history analysis, Kaveh et al. presented a new objective function for optimal design of Buckling Restrained Braced Frames (BRBFs) [26]. Hosseini et al. calculated the reliability index of four transmission line towers using four metaheuristic algorithms based on the displacement of the nodes, and compared the results with Monte Carlo Simulations (MCS) [27]. To increase response robustness and decrease weight, Hosseini et al optimized two space trusses based on modulus of elasticity, yield stress, and cross-sectional uncertainties [28]. According to Hosseini et al, the reliability indexes of Deterministic Design Optimization (DDO) for large dome trusses and Reliability-Based Design Optimization (RBDO) were compared for three large-scale dome trusses [29].

There are several parameters in the EVPS algorithm, including α , p , w_1 , w_2 , $HMCR$, PAR , $Neighbor$ and $Memory_size$, which are experimentally determined; however, these parameters are considered specific values by default. This study investigates the effects of each parameter on the obtained optimal solution and proposes a method for adjusting them. These parameters can be adjusted to improve the convergence speed and accuracy of the EVPS algorithm, as well as its ability to escape local optima. This method is known as a Self-Adaptive EVPS algorithm (SA-EVPS). This method was evaluated using four examples, including three benchmarked functions, namely F5, F6 and F13, and a 72 bar spatial truss structure, in order to optimize and compare the results of EVPS and SA-EVPS.

The paper is organized as follows: The introduction is presented in Section one. Section two provides a brief explanation of the EVPS algorithm. In section three, SA-EVPS is discussed. The fourth section contains four benchmark problems. The final section of the paper presents the conclusion.

2. A BRIEF EXPLANATION OF THE EVPS ALGORITHM [29]

Kaveh et al. presented the EVPS algorithm [30], which is an improved version of the VPS algorithm that was presented in 2018 [31]. As of now, the EVPS algorithm is being used successfully in structural optimization topics. The following performance characteristics are associated with this algorithm:

In the first instance, the permissible range of the initial population created by Eq. (1) must be considered.

$$x_i^j = x_{min} + rand.(x_{max} - x_{min}) \quad (1)$$

where x_i^j is the j th variable of the i th particle; x_{max} and x_{min} are the upper and lower

bounds of design variables in the search space, respectively. An additional parameter, called memory, maintains the number of memory sizes from the best positions achieved by the population. The effect of damping level on vibration is described by equation (2).

$$D = \left(\frac{iter}{iter_{max}} \right)^{-\alpha} \quad (2)$$

where $iter$ is the current number of iterations; $iter_{max}$ is the total number of iterations and α is a parameter with a constant value; ± 1 is used randomly. Finally, the new positions of the population are updated by Eq. (3).

$$x_i^j = \begin{cases} \left[D.A.rand1 + OHB^j \right] & (a) \\ \left[D.A.rand2 + GP^j \right] & (b) \\ \left[D.A.rand3 + BP^j \right] & (c) \end{cases} \quad (3)$$

where OHB , GP , and BP are determined independently for each of the variables, and A is defined as follows:

$$A = \begin{cases} (\pm 1)(OHB^j - x_i^j) & (a) \\ (\pm 1)(GP^j - x_i^j) & (b) \\ (\pm 1)(BP^j - x_i^j) & (c) \end{cases} \quad (4)$$

$$\omega_1 + \omega_2 + \omega_3 = 1$$

The coefficients ω_1 , ω_2 , and ω_3 are the relative importance for OHB , GP , and BP , respectively; $rand1$, $rand2$, and $rand3$ are random numbers uniformly distributed in the $[0, 1]$ range. It should be noted that what was discussed is only a summary of the EVPS algorithm, and the author may wish to consult Kaveh et al's study in order to obtain a more complete explanation [30].

3. SELF-ADAPTIVE EVPS ALGORITHM (SA-EVPS)

In the previous section, it was discussed that the EVPS algorithm makes use of eight variables, including α , p , w_1 , w_2 , $HMCR$, PAR , $Neighbor$, and $Memory_size$, which are experimentally determined. In spite of the fact that these parameters are considered specific values by default in the EVPS algorithm, they are set as constants of 0.05, 0.2, 0.3, 0.3, 0.95, 0.1, 0.1 and 4, respectively. Search accuracy, exploration and exploit phases, convergence speed, and overall algorithm behavior are controlled by the EVPS parameters. As a result, all of these parameters have a significant impact on the behavior of the method. All eight parameters mentioned above are also optimized before the main optimization takes place. First, all 8 parameters are optimized for the desired problem using the EVPS algorithm, and then the main optimization is conducted. A schematic illustration of the SA-EVPS algorithm can be found in Fig. 1.

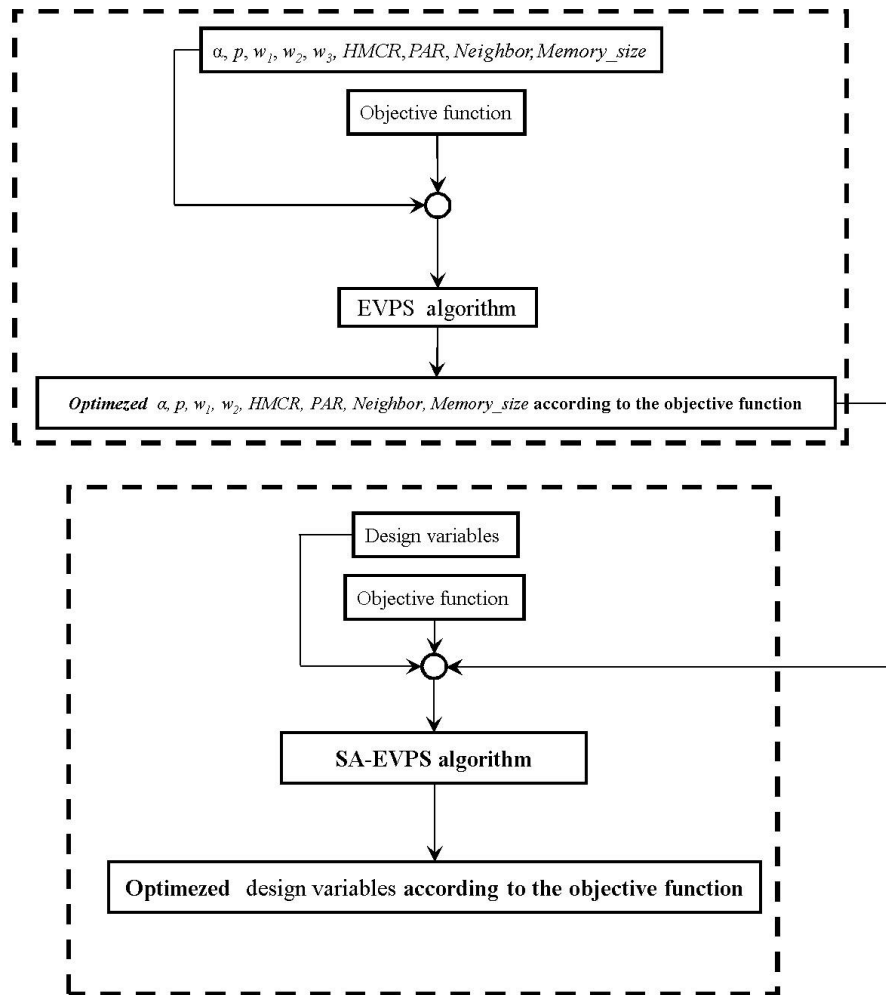


Figure 1. schematic illustration of the SA-EVPS algorithm

4. NUMERICAL EXAMPLES

In this section, a number of numerical examples including benchmarked functions, namely F_5 , F_6 , and F_{13} , and the 72 bar spatial truss structure are compared using the EVPS and SA-EVPS algorithms. In the optimization process, 30 independent runs are conducted for each example. In all problems, the population size is 30. In the EVPS algorithm α , p , w_1 , w_2 , $HMCR$, PAR , $Neighbor$ and $Memory_size$ are 0.05, 0.2, 0.3, 0.3, 0.95, 0.1, 0.1, and 4, respectively.

4.1 The 72 bar spatial truss structure

Based on the 72-bar spatial truss structure shown in Fig 2, the elements can be classified into sixteen design groups:

(1) A1_A4, (2) A5_A12, (3) A13_A16, (4) A17_A18, (5) A19_A22, (6) A23_A30, (7) A31_A34, (8) A35_A36, (9) A37_A40, (10) A41_A48, (11) A49_A52, (12) A53_A54, (13) A55_A58, (14) A59_A66 (15), A67_A70, and (16) A71_A72.

It is assumed that the density of the material is 0.1 lb/in^3 and the modulus of elasticity is 10,000 ksi. Members are subjected to a stress limit of 25 ksi. Nodes are subject to displacement limits of 0.25 inches. For each member, the minimum cross-sectional area is 0.10 in^2 , and the maximum cross-sectional area is 4.00 in^2 . The loading conditions are as follows:

1. Node 17 is loaded with 5, 5 and -5 kips in the x, y, and z directions, respectively.
2. There is a load of -5 kips in the z direction at nodes 1, 2, 3 and 4.

Fig. 3 illustrates the effects of changing each of the parameters on the EVPS algorithm by showing the best, worst, and mean answers along with the standard deviation associated with each value. It is significant to note that each point in this figure is the result of 30 independent runs. As can be seen in this figure, each parameter has a significant impact on the quality of the answer. According to the figures, some parameters have a greater effect than others (such as α , w_1 , p , PAR, and HMCR).

Table 1 shows the parameters of the SA-EVPS algorithm that are self-adaptive (optimized). Table 2 shows the lightest weight, the worst weight, the mean weight, and the standard deviation of 30 independent runs obtained by EVPS and SA-EVPS algorithms. SA-EVPS algorithm has achieved better results than EVPS algorithm. The convergence diagrams for EVPS and SA-EVPS algorithms for 30 independent runs are shown in Fig. 4 (Logarithmic scale was selected for the vertical axis due to an issue with visualizations skewing towards very small values over a very broad range of values).

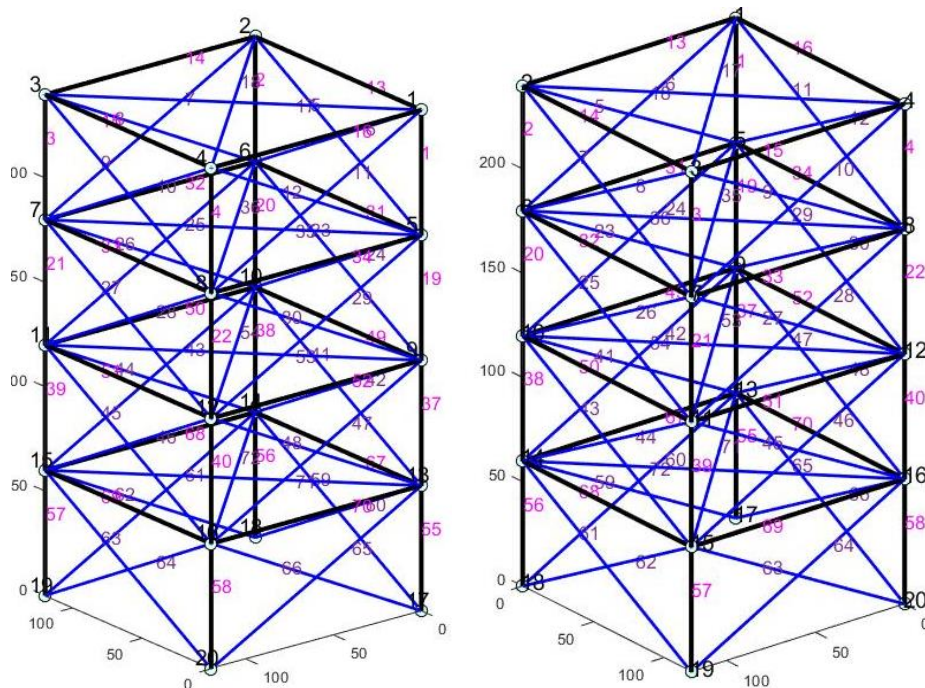


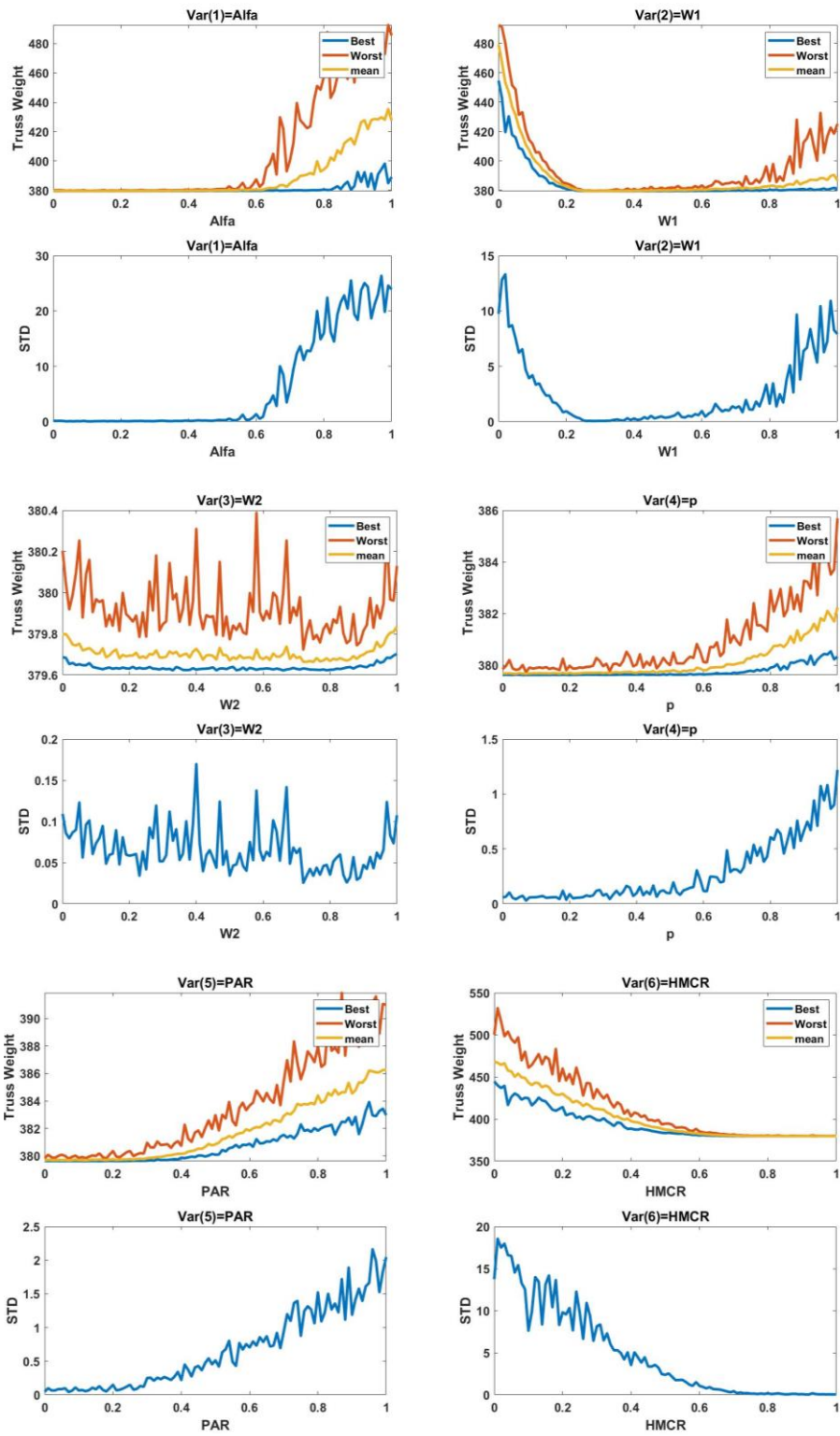
Figure 2. illustration of the 72-bar spatial truss from two view

Table 1: SA-EVPS algorithm parameters that are self-adaptive (optimized) for 72-bar spatial truss

| truss | | |
|-------|-------------|------------|
| | Parameter | Value |
| 1 | α | 0.06744712 |
| 2 | p | 0.2903912 |
| 3 | w_1 | 0.7941491 |
| 4 | w_2 | 0.2115948 |
| 5 | HMCR | 0.08632188 |
| 6 | PAR | 0.8558247 |
| 7 | Neighbor | 0.8414693 |
| 8 | Memory_size | 1 |

Table 2: Evaluation of EVPS and SA-EVPS results for the 72-bar spatial truss

| Element Group | | Optimal cross-sectional areas (in ²) | |
|--------------------|---------|--|-------------|
| | | EVPS | SA-EVPS |
| 1 | A1-A4 | 0.156026 | 0.1563854 |
| 2 | A5-A12 | 0.550565 | 0.5474971 |
| 3 | A13-A16 | 0.41266 | 0.4081775 |
| 4 | A17-A18 | 0.568612 | 0.5751029 |
| 5 | A19-A22 | 0.536759 | 0.5224397 |
| 6 | A23-A30 | 0.519986 | 0.5116629 |
| 7 | A31-A34 | 0.1 | 0.1000004 |
| 8 | A35-A36 | 0.100734 | 0.1002537 |
| 9 | A37-A40 | 1.26445 | 1.2693775 |
| 10 | A41-A48 | 0.508508 | 0.512734 |
| 11 | A49-A52 | 0.100002 | 0.1 |
| 12 | A53-A54 | 0.1 | 0.1000002 |
| 13 | A55-A58 | 1.858562 | 1.8915552 |
| 14 | A59-A66 | 0.511243 | 0.5129524 |
| 15 | A67-A70 | 0.1 | 0.1000001 |
| 16 | A71-A72 | 0.100001 | 0.1 |
| Best weight (lb) | | 379.6433149 | 379.6288237 |
| Worst weight (lb) | | 380.4062092 | 380.003324 |
| Average weight(lb) | | 379.86586 | 379.7419802 |
| STD | | 0.195520567 | 0.101362697 |



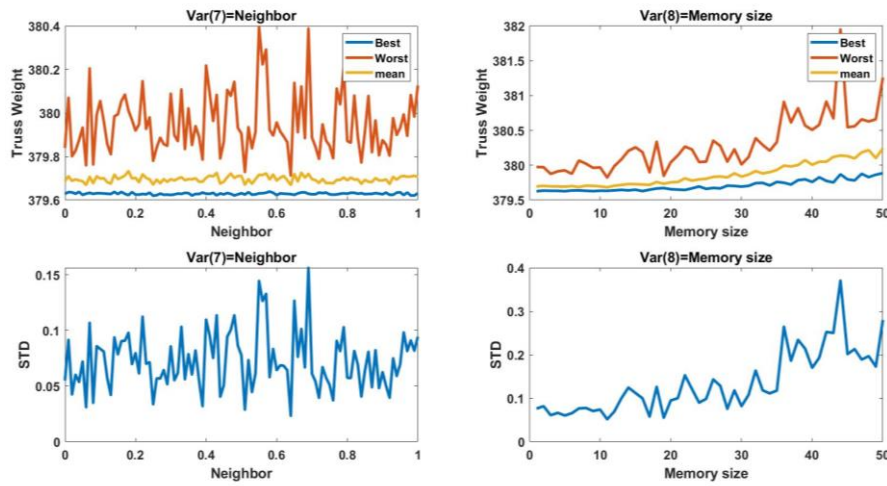
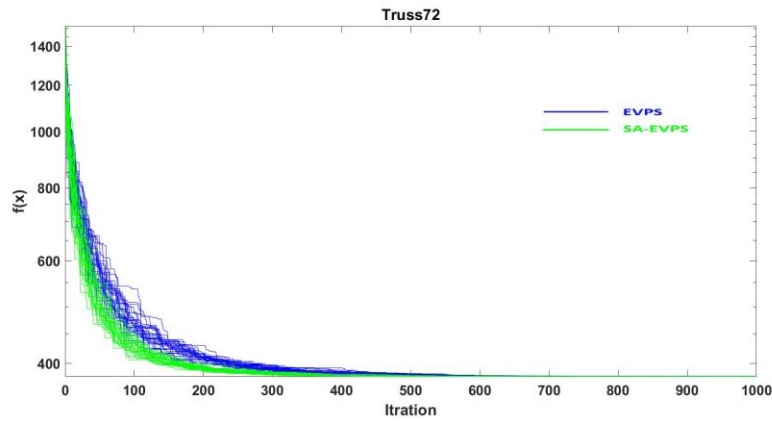
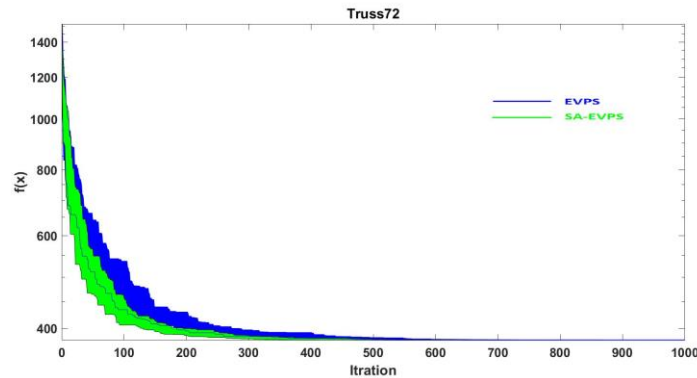


Figure 3. illustration the effects of changing each of the parameters on the EVPS algorithm for the 72-bar spatial truss



(a)



(b)

Figure 4. Convergence curves for the spatial 72-bar spatial truss of 30 independent runs for EVPS and SA-EVPS. (a) graph in linear form, (b) graph in Solid form

4.2 Three classical benchmarked functions

This section compares the SA-EVPS algorithm with the EVPS algorithm using three benchmark functions. Many researchers use these benchmark functions as classical functions [17]. Although these benchmark functions are simple, they were chosen to evaluate the performance of the SA-EVPS algorithm. Table 3 shows the benchmark functions. Dim indicates the dimension of the function, Range is the bounds of the function's search space, and f_{\min} is the optimum. Figs. 5 to 7 illustrate the functions of table 3. Based on three classical benchmarks, Table 4 shows the parameters of the SA-EVPS algorithm that are self-adaptive (optimized). According to Table 5, the optimal answer, the worst, the mean answer, and the standard deviation for 30 independent runs were obtained using the EVPS and SA-EVPS algorithms. It has been demonstrated that the SA-EVPS algorithm has achieved better results than the EVPS algorithm. Figs. 8 to 10 illustrate the convergence diagrams for the EVPS and SA-EVPS algorithms over 30 independent runs. (Logarithmic scale was selected for the vertical axis due to an issue with visualizations skewing towards very small values over a very broad range of values.)

Table 3: the classical benchmark functions

| Function | Dim | Range | fmin |
|---|-----|------------|------|
| $f_5(x) = \sum_{i=1}^{n-1} [100(x_{i+1} - x_i^2)^2 + (x_i - 1)^2]$ | 30 | [-30,30] | 0 |
| $f_6(x) = \sum_{i=1}^n ([x_i + 0.5])^2$ | 30 | [-100,100] | 0 |
| $f_{15}(x) = 0.1 \left\{ \sin^2(3\pi x_1) + \sum_{i=1}^n (x_i - 1)^2 [1 + \sin^2(3\pi x_i + 1)] + (x_n - 1)^2 [1 + \sin^2(2\pi x_n)] \right\} + \sum_{i=1}^n u(x_i, 5, 100, 4)$ | 30 | [-50,50] | 0 |

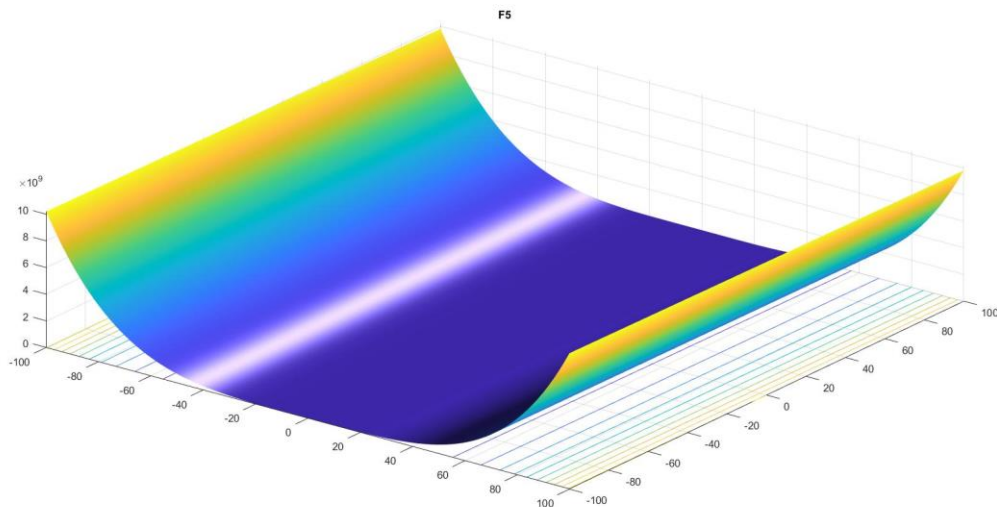


Figure 5. The F_5 function of Table 3

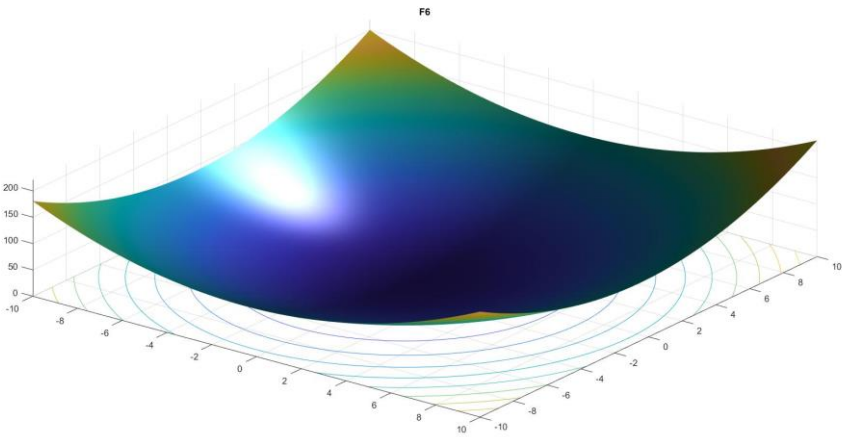


Figure 6. The F_6 function of Table 3

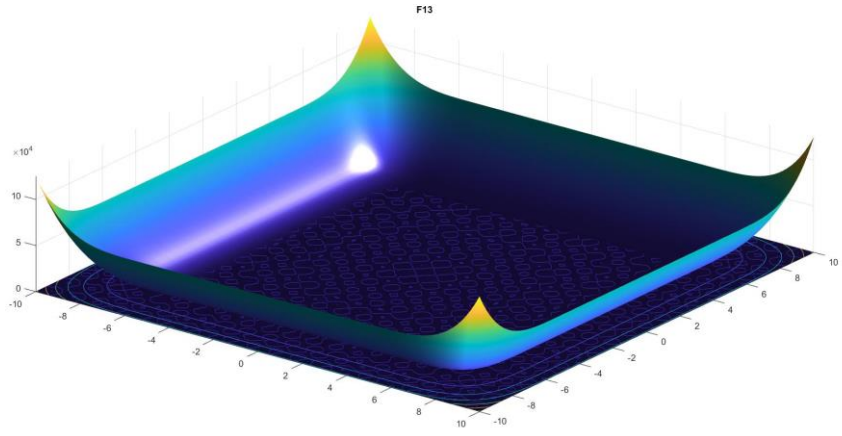


Figure 7. The F_{13} function of Table 3

Table 4: SA-EVPS algorithm parameters that are self-adaptive (optimized) for three classical benchmarked functions

| Parameter | | F_5 | F_6 | F_{13} |
|-----------|-------------|------------|----------|-----------|
| | | Value | Value | Value |
| 1 | α | 0.06744712 | 0.029785 | 0.02728 |
| 2 | p | 0.2903912 | 0.38725 | 0.45861 |
| 3 | w_1 | 0.7941491 | 0.56282 | 0.45134 |
| 4 | w_2 | 0.2115948 | 0.48619 | 0.0038396 |
| 5 | HMCR | 0.08632188 | 0.51944 | 0.53381 |
| 6 | PAR | 0.8558247 | 0.58075 | 0.31759 |
| 7 | Neighbor | 0.8414693 | 0.88721 | 0.64264 |
| 8 | Memory_size | 1 | 3 | 1 |

Table 5: Evaluation of EVPS and SA-EVPS results for the 72-bar spatial truss

| | F ₅ | | F ₆ | | F ₁₃ | |
|----------------|----------------|------------|----------------|------------|-----------------|------------|
| | EVPS | SA-EVPS | EVPS | SA-EVPS | EVPS | SA-EVPS |
| Best weight | 37.7759788 | 0.17620538 | 5.3183E-05 | 6.715E-19 | 0.00017724 | 5.3672E-15 |
| Worst weight | 2606.9576 | 428.554252 | 0.12163476 | 7.4583E-11 | 1.59782395 | 3.64141345 |
| Average weight | 357.777465 | 112.213601 | 0.00513199 | 2.6297E-12 | 0.07729826 | 0.51374684 |
| STD | 535.464537 | 97.6568764 | 0.0216576 | 1.3367E-11 | 0.28864004 | 0.90305428 |

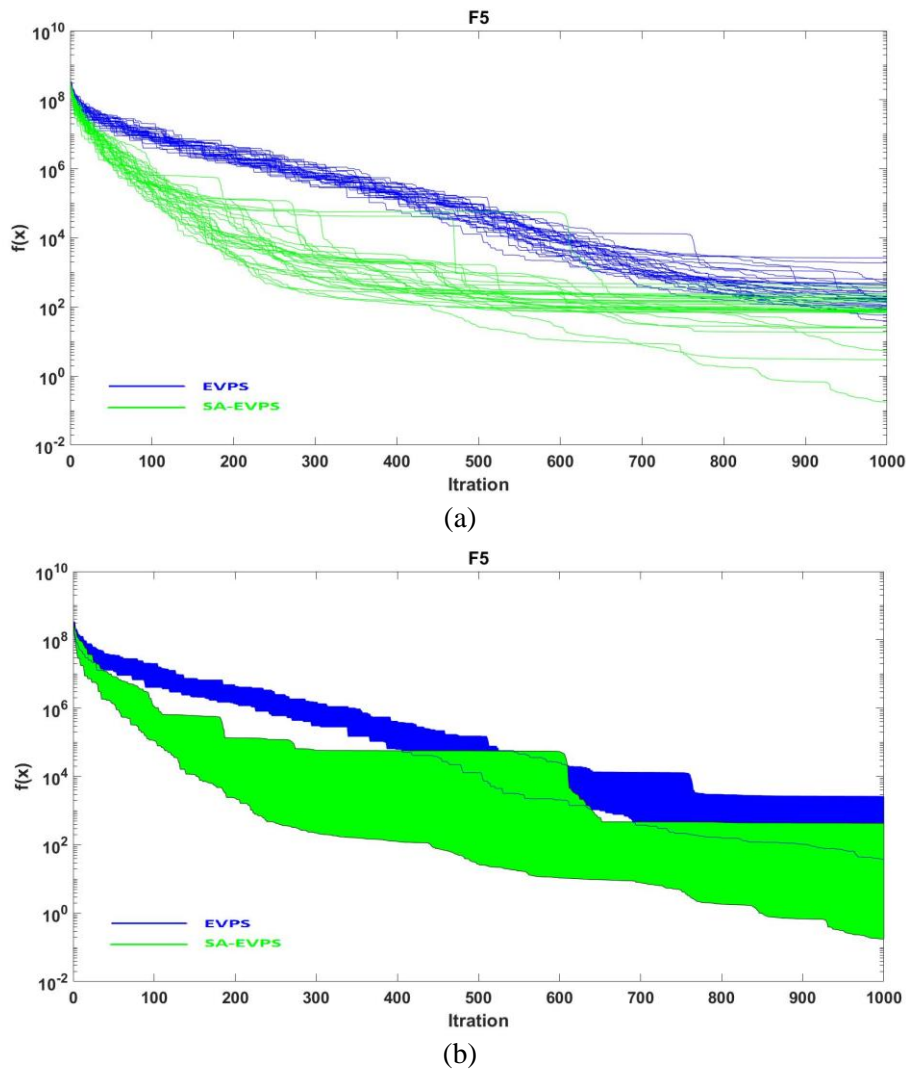
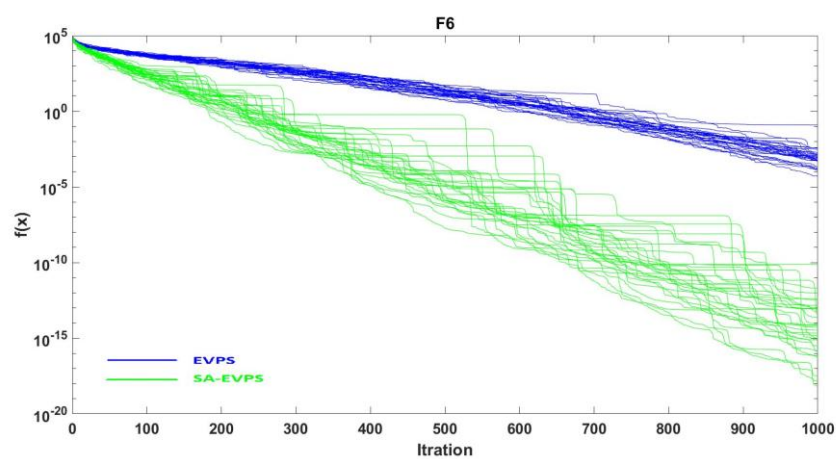
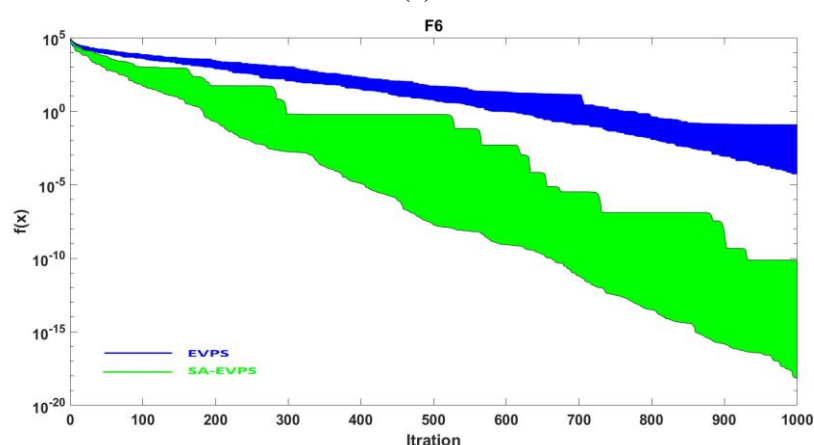


Figure 8. Convergence curves for 30 independent runs of the F_5 function are shown in Table 3. (a) graph in linear form, (b) graph in Solid form

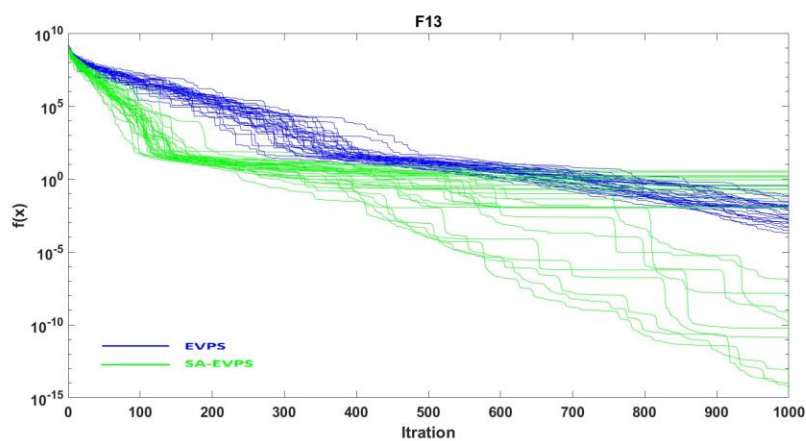


(a)



(b)

Figure 9. Convergence curves for 30 independent runs of the F_6 function are shown in Table 3.
(a) graph in linear form, (b) graph in solid form



(a)

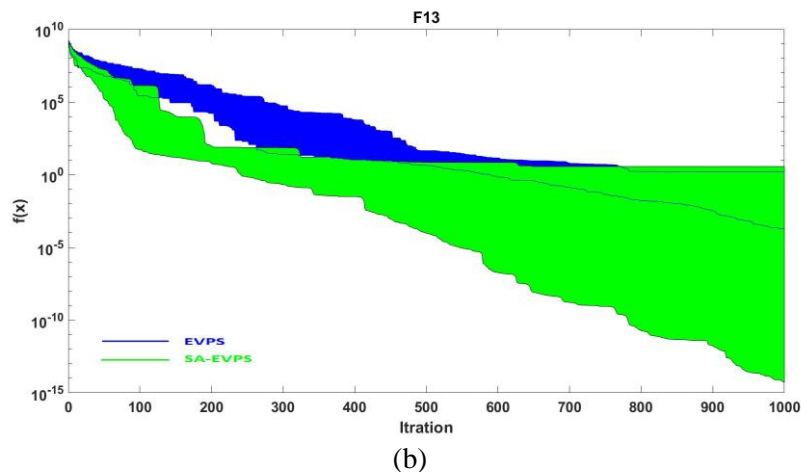


Figure 10. Convergence curves for 30 independent runs of the F_{13} function are shown in Table 3.
(a) graph in linear form, (b) graph in Solid form

5. CONCLUSION

The EVPS algorithm has been successfully applied to a variety of optimization problems to date. As with many metaheuristic algorithms, the EVPS algorithm comprises parameters such as α , p , w_1 , w_2 , $HMCR$, PAR , $Neighbor$ and $Memory_size$ that are experimentally determined. These parameters are usually recommended by the algorithm's provider by default. The effect of each of these parameters on the optimal solution was investigated in this study. This investigation led to the development of a self-adaptive process known as the SA-EVPS algorithm. Two EVPS and SA-EVPS algorithms were examined for the 72 bar spatial truss structure and three classical benchmarked functions, and the results indicated that the SA-EVPS algorithm performed better in terms of convergence speed and solution quality. There is a suggestion to use the SA-EVPS algorithm for other types of optimization problems.

REFERENCES

1. Kaveh A, Rahami H. Analysis, design and optimization of structures using force method and genetic algorithm, *Int J Numer Meth Eng* 2006; **65**(10): 1570-84.
2. Kaveh A, Talatahari S. A charged system search with a fly to boundary method for discrete optimum design of truss structures, *Asian J Civil Eng* 2010; **11**: 277-93.
3. Kaveh A, Mahdavi VR. Colliding bodies optimization: a novel meta-heuristic method, *Comput Struct* 2014; **139**: 18-27.
4. Kaveh A, Zolghadr A. A novel meta-heuristic algorithm: tug of war optimization, *Int J Optim Civil Eng* 2016; **6**(4): 469-92.
5. Kaveh A, Bakhshpoori T. An accelerated water evaporation optimization formulation for

- discrete optimization of skeletal structures, *Comput Struct* 2016; **177**: 218-28.
6. Kaveh A, Farhoudi N. A new optimization method: Dolphin echolocation, *Adv Eng Softw* 2013; **59**: 53-70.
 7. Kaveh A, Hoseini Vaez SR, Hosseini P, Fallah N. Detection of damage in truss structures using Simplified Dolphin Echolocation algorithm based on modal data, *Smart Struct Syst* 2016; **18**(5): 983-1004.
 8. Kaveh A, Hoseini Vaez SR, Hosseini P. Modified dolphin monitoring operator for weight optimization of frame structures, *Period Polytech Civil Eng* 2017; **61**(4): 770-9.
 9. Qin AK, Huang VL, Suganthan PN. Differential evolution algorithm with strategy adaptation for global numerical optimization, *IEEE Transact Evolut Computat* 2008; **13**(2): 398-417.
 10. Jalili S, Kashan AH, Hosseinzadeh Y. League championship algorithms for optimum design of pin-jointed structures, *J Comput Civil Eng* 2016; **31**(2): 04016048.
 11. Rao RV, Savsani VJ, Vakharia D. Teaching-learning-based optimization: a novel method for constrained mechanical design optimization problems, *Comput-Aided Des* 2011; **43**(3): 303-15.
 12. Bechikh S, Chaabani A, Said LB. An efficient chemical reaction optimization algorithm for multiobjective optimization, *IEEE Transact Cybernet* 2014; **45**(10): 2051-64.
 13. Mirjalili S. SCA: A sine cosine algorithm for solving optimization problems, *Knowl-Based Syst* 2016; **96**: 120-33.
 14. Shabani A, Asgarian B, Salido M, Gharebaghi SA. Search and rescue optimization algorithm: A new optimization method for solving constrained engineering optimization problems, *Expert Syst Applicat* 2020; **161**: 113698.
 15. Kaur A, Kumar Y. A new metaheuristic algorithm based on water wave optimization for data clustering, *Evolut Intell* 2022; **15**(1): 759-83.
 16. Hashim FA, Houssein EH, Hussain K, Mabrouk MS, Al-Atabany W. Honey Badger Algorithm: New metaheuristic algorithm for solving optimization problems, *Mathemat Comput Simulat* 2022; **192**: 84-110.
 17. Mirjalili S, Mirjalili SM, Lewis A. Grey wolf optimizer, *Adv Eng Softw* 2014; **69**: 46-61.
 18. Kaveh A, Hoseini Vaez SR, Hosseini P. Enhanced vibrating particles system algorithm for damage identification of truss structures, *Sci Iran* 2019; **26**(1): 246-56.
 19. Kaveh A, Hoseini Vaez SR, Hosseini P, Bakhtiari M. Optimal Design of Steel Curved Roof Frames by Enhanced Vibrating Particles System Algorithm, *Period Polytech Civil Eng* 2019; **63**(4): 947-60.
 20. Hoseini Vaez SR, Mehanpour H, Fathali MA. Reliability assessment of truss structures with natural frequency constraints using metaheuristic algorithms, *J Build Eng* 2020; **28**: 101065.
 21. Fathi H, Hoseini Vaez SR, Zhang Q, Alavi AH. A new approach for crack detection in plate structures using an integrated extended finite element and enhanced vibrating particles system optimization methods, *Struct* 2021; **29**: 638-51.
 22. Kaveh A, Hoseini Vaez SR, Hosseini P, Fathali MA. Heuristic operator for reliability assessment of frame structures, *Period Polytech Civil Eng* 2021; **65**(3): 702-16.
 23. Kaveh A, Khosravian M. Size/layout optimization of truss structures using vibrating particles system meta-heuristic algorithm and its improved version, *Period Polytech Civil*

- Eng* 2022; **66**(1): 1-17.
24. Kaveh A, Hoseini Vaez SR, Hosseini P, Fathali MA. A new two-phase method for damage detection in skeletal structures, *Iran J Sci Technol, Transact Civil Eng* 2019; **43**(1): 49-65.
 25. Hoseini Vaez SR, Fathali MA, Mehanpour, H. A two-step approach for reliability-based design optimization in power transmission line towers, *Int J Interact Des Manufact (IJIDeM)* 2022: 1-25.
 26. Kaveh A, Hoseini Vaez SR, Hosseini P, Abedini H. Weight minimization and energy dissipation maximization of braced frames using EVPS algorithm, *Int J Optim Civil Eng* 2020; **10**(3): 513-29
 27. Hosseini P, Hoseini Vaez SR, Fathali MA, Mehanpour H. Reliability assessment of transmission line towers using metaheuristic algorithms, *Int J Optim Civil Eng* 2020; **10**(3): 531-55.
 28. Hosseini P, Kaveh A, Hoseini Vaez SR. Robust design optimization of space truss structures, *Int J Optim Civil Eng*; **12**(4): 595-608.
 29. Hosseini P, Kaveh A, Hoseini Vaez SR. The optimization of large-scale dome trusses on the basis of the probability of failure, *Int J Optim Civil Eng* 2022; **12**(3): 457-75.
 30. Kaveh A, Hoseini Vaez SR, Hosseini P. MATLAB code for an enhanced vibrating particles system algorithm, *Int J Optim Civil Eng* 2018; **8**(3): 401-14.
 31. Kaveh A, Ilchi Ghazaan M. Vibrating particles system algorithm for truss optimization with multiple natural frequency constraints, *Acta Mech* 2017; **228**(1): 307-22.